

the parity selection rules. However, having the frequencies close to those of the electronic (magnon) transitions, the Raman phonons may mix up with the electronic excitations and become allowed even in the electric dipolar approximation. Just the results of the magnetic susceptibility studies [7] show that in addition to the magnon frequencies 67 and 79.3 cm^{-1} , this region of the CoWO_4 spectrum must contain electronic transitions at ~ 290 and $\sim 300\text{ cm}^{-1}$. The strong effect of the external field $H_0 \parallel Z$ on the frequencies of some of the bands requires special consideration.

REFERENCES

- [1] R. O. Keeling, "Structure of NiWO_4 ," *Acta Crystallogr.*, vol. 10, pp. 209-213, Sept. 1957.
- [2] D. Ulkü, "Investigation of crystal and magnetic structure of ferberit FeWO_4 ," *Z. Kristallogr.*, vol. 124, pp. 192-219, June 1967.
- [3] H. Weitzel, "Magnetic structure of CoWO_4 , NiWO_4 and CuWO_4 ," *Solid State Commun.*, vol. 8, pp. 2071-2072, Dec. 1970.
- [4] L. G. Van Uitert *et al.*, "Magnetic properties of a number of divalent transition metal tungstates, molybdates and titanates," *J. Phys. Chem. Solids*, vol. 25, pp. 1447-1451, Dec. 1964.
- [5] A. I. Zvyagin and E. N. Khats'ko, "Magnetic properties of cobalt tungstate," *Fiz. Tverd. Tela*, vol. 12, pp. 314-316, Jan. 1970.
- [6] I. V. Skorobogatova and A. I. Zvyagin, "The effect of magnetic ordering on the absorption spectrum of NiWO_4 ," *Opt. Spectrosc.*, vol. 33, pp. 594-596, Sept. 1972.
- [7] E. N. Khats'ko and A. I. Zvyagin, "Crystalline field of low symmetry effect on magnetic properties of CoWO_4 ," *Proc. Phys. Tech. Inst. Low Temp. (Kharkov)*, vol. 18, pp. 3-14, Nov. 1972.
- [8] A. A. Galkin, A. D. Prokhorov, and G. A. Tsintsadze, "Hyperfine structure of EPR Co^{2+} in ZnWO_4 ," *Fiz. Tverd. Tela*, vol. 8, p. 3674, Nov. 1966.
- [9] R. J. Riggs and K. J. Standley, "The electron spin resonance of Cu^{2+} and Ni^{2+} ions in zinc tungstate," *J. Phys.*, vol. C2, pp. 992-997, July 1969.
- [10] A. I. Zvyagin *et al.*, "Magnetic properties and EPR of nickel tungstate," *Proc. Phys. Tech. Inst. Low Temp. (Kharkov)*, vol. 18, pp. 67-74, Nov. 1972.
- [11] V. N. Kitaev, M. P. Kaschenko, and L. V. Kurbatov, "Single ion anisotropy effect on the spin wave spectrum," *Fiz. Tverd. Tela*, vol. 15, pp. 2292-2298, Aug. 1973.
- [12] V. M. Naumenko, V. I. Fomin, and V. V. Eremenko, "Far infrared grating spectrometer," *Prib. Tekh. Eksp.*, pp. 223-224, Sept.-Oct. 1967.
- [13] V. M. Gredescul, S. A. Gredescul, V. V. Eremenko, and V. M. Naumenko, "Magnetization and resonance in orthorhombic antiferromagnets with the Dzyaloshinsky interaction (CoWO_4)," *J. Phys. Chem. Solids*, vol. 33, pp. 859-880, Apr. 1972.
- [14] V. I. Kut'ko, V. M. Naumenko, and A. I. Zvyagin, "Absorption spectrum of nickel tungstate in far IR," *Fiz. Tverd. Tela*, vol. 14, pp. 3436-3438, Nov. 1972.
- [15] V. I. Kut'ko *et al.*, "Vibrational spectra of monoclinic tungstates," *Proc. Phys. Tech. Inst. Low Temp. (Kharkov)*, vol. 5, pp. 203-219, Oct. 1969.
- [16] V. V. Eremenko, Y. G. Litvinenko, and Y. A. Popkov, "Light absorption and combination scattering in antiferromagnetic NiWO_4 ," presented at the 19th Annu. Conf. Magnetism, USA, Rep. 4C-2, Nov. 1973.

Far-Infrared Properties of Interacting Donors in Antimony-Doped Germanium

KAZUO YOSHIHIRO, MADOKA TOKUMOTO, AND CHIKAKO YAMANOUCHI

Abstract—Absorption and photoconductivity of $337\text{-}\mu\text{m}$ radiation in Sb-doped Ge with excess donor concentrations ranging from 1.2×10^{16} to $3.6 \times 10^{17}\text{ cm}^{-3}$ have been investigated at liquid-He temperatures. The result suggests the existence of a "delocalized" excited state between the conduction band and the donor ground state which arises from the overlapping of donor wave functions.

I. INTRODUCTION

ESSENTIAL PARTS of information about the impurity state in semiconductors can be obtained through studying their far-infrared properties. Investigations in this field on impurity centers in semiconductors have been restricted so far to the point where the impurity

concentration is so low that the interaction between centers can be ignored.

The purpose of the present investigation is to study the far-infrared properties in semiconductors in which the impurity centers are interacting. One of the most interesting problems is impurity conduction in the intermediate impurity-concentration region where the resistivity is characterized by an activation energy ϵ_2 at low temperatures [1], as is shown in Fig. 1. The activation energy ϵ_2 depends strongly on the impurity concentration [1], magnetic field [2]-[6], deformation [7]-[10], and compensation [11], [12] in contrast to the donor ionization energy ϵ_1 and the activation energy ϵ_3 for hopping-type conduction. These behaviors of ϵ_2 have been understood in terms of the change in the overlapping of donor wave functions, and ϵ_2 has been supposed to be an energy needed to excite electrons from the donor ground state into the

Manuscript received May 7, 1974.

The authors are with the Electrotechnical Laboratory, Tanashi, Tokyo, Japan.

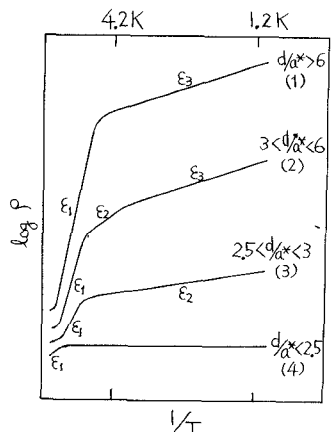


Fig. 1. Temperature dependence of the resistivity in different regions of impurity concentration. a^* : effective Bohr radius of the localized wave function. d : mean distance between donors. For Sb-doped Ge, (1): $N_D - N_A < 1 \times 10^{16} \text{ cm}^{-3}$; (2): $N_D - N_A = 1 \sim 7 \times 10^{16} \text{ cm}^{-3}$; (3): $N_D - N_A = 7 \sim 13 \times 10^{16} \text{ cm}^{-3}$; (4): $N_D - N_A > 13 \times 10^{16} \text{ cm}^{-3}$.

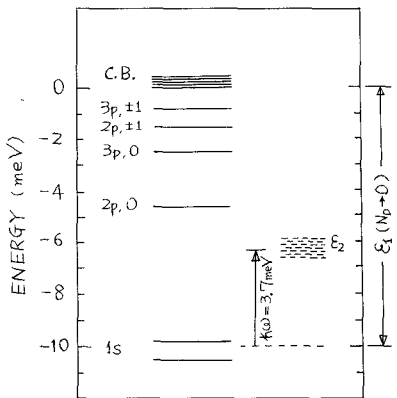


Fig. 2. Energy-level schemes of an isolated Sb impurity and a delocalized state in Ge. Also shown is the photon energy of wavelength $337 \mu\text{m}$ measured from the center of gravity of the ground state.

unbound state in which a current can flow [1], [7]. The present study is aimed at observing the optical transition which would occur if this picture were real.

The absorption and photoconductive response of a monochromatic $337\text{-}\mu\text{m}$ radiation produced by an HCN laser [13] has been investigated in n-Ge single crystals. The excess donor concentration ranges from 1.2×10^{16} to 3.6×10^{17} Sb atoms/ cm^3 . No compensating impurity was intentionally doped. For the samples investigated, ϵ_2 decreases from 5.8 to 0.1 meV as the concentration is changed from 1.2×10^{16} to 1.1×10^{17} Sb atoms/ cm^3 .

Fig. 2 shows a schematic diagram of energy levels of an isolated Sb donor in Ge. The energy separation between the ground and the first excited states of an isolated donor is larger than the photon energy of $337\text{-}\mu\text{m}$ radiation, 3.7 meV. If an optical transition is induced by the $337\text{-}\mu\text{m}$ radiation in an actual crystal of Sb-doped Ge at temperatures near $T = 0$, it would be an indication of the appreciable effect of the overlapping of donor wave functions. An HCN laser or other monochromatic sources with radiation between $300 \mu\text{m}$ and 1 mm in wavelength are

particularly suited to investigate interactions between impurity centers in semiconductors.

II. EXPERIMENTAL

The arrangement for the optical and electrical measurements is shown in Fig. 3. The radiation of $337 \mu\text{m}$ from the HCN laser was chopped at 20 Hz by a mechanical light chopper and was introduced into the cryostat through a cupro-nickel light pipe of 12-mm ID. The radiation was concentrated on the sample by a conical light pipe which is similar to the one described by Williamson [14]. A piece of black polyethylene sheet 0.1 mm thick was placed at the lower end of the light cone to cut out the room-temperature radiation.

The radiation transmitted through the sample was detected by an n-InSb photoconductive detector placed just behind the sample. The signal voltage of 20 Hz which was generated across the detector or the sample was fed into a PAR Model HR-8 lock-in amplifier with type A or D preamplifier. The power of radiation was monitored by the Golay cell with a silicon window continuously during the experiments. The sample and detector were immersed in liquid He to avoid the possible temperature rise on irradiation.

The n-InSb photoconductive detector was a $0.6 \times 1.0 \times 7\text{-mm}^3$ block with a pair of potential arms and was cut from a single crystal of grade 67S obtained from Cominco. A typical detector had a resistivity of $0.066 \Omega\text{-cm}$ and a mobility of $8.6 \times 10^5 \text{ cm}^2/\text{V}\cdot\text{s}$ at 77K.

For the InSb detector and the samples investigated, the photoresponses were proportional to the power of incident radiation which was below milliwatt level.

The samples were bridge-shaped and about $10 \times 1 \times (0.05 - 1.0) \text{ mm}^3$ in size. The characteristics of the samples are listed in Table I. The excess donor concentration $N_D - N_A$ was obtained from the Hall coefficient R_{300} measured at room temperature with a magnetic field of 7 kOe and the relation $N_D - N_A = 1/eR_{300}$. The compensation ratio N_A/N_D was estimated at less than 5 percent. The activation energy ϵ_2 for the respective samples was obtained from the resistivity measurements below 20 K.

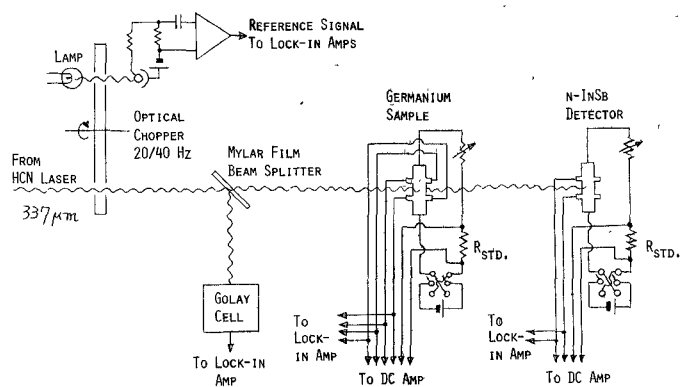


Fig. 3. Schematic diagram of the arrangement for optical measurement.

TABLE I
CHARACTERISTICS OF SAMPLES

CODE OF SAMPLES	$N_D - N_A$ ($10^{16} \cdot \text{cm}^{-3}$)	$\rho(300\text{K})$ ($10^{-2} \Omega \cdot \text{cm}$)	$\rho(4.2\text{K})$ ($\Omega \cdot \text{cm}$)	ϵ_2 (meV)
1171-h3	0.0065	4620	—	
S0101-1-5	1.21	12.21	8.56×10^4	5.82
S0101-1-4	1.29	12.26	5.13×10^4	5.51
194-25	1.73	10.72	2.34×10^4	4.94
194-31	2.02	9.57	1.52×10^4	4.52
194-33	2.20	8.60	9.76×10^3	3.90
S0101-2-2	2.50	6.69	4.31×10^3	3.82
S0101-2-1	2.40	6.64	4.06×10^3	3.58
S0101-2'-1	2.76	6.76	2.04×10^3	3.24
S0101-2"-1	3.30	5.85	6.09×10^2	2.74
S0101-3-1	3.97	5.33	2.17×10^2	2.45
S0101-4-1	4.86	4.72	5.86×10^1	1.87
S0101-4-3	5.00	4.65	3.46×10^1	1.60
S0101-4-4	5.20	4.22	2.00×10^1	1.48
S0101-5-1	5.96	4.04	9.83×10^0	1.13
292-29a	6.68	3.67	1.99×10^0	0.49
S0101-5-4b	7.45	3.15	1.09×10^0	0.34
S0101-6-2a	8.98	2.80	4.58×10^{-1}	0.16
S0101-6-4	10.0	2.54	2.63×10^{-1}	≈ 0.1
S0101-6-3'a	10.5			
S0101-7-4	12.3	2.27	1.49×10^{-1}	≈ 0
S0101-7-2a	11.9	2.21		
192-47b	13.0			
S0101-8-1'	13.2	2.21		
S0101-8-1	14.0	1.91	8.48×10^{-2}	0
292-31a	14.3			
192-52d	15.0			
187-2ha	19.8	1.72	4.78×10^{-2}	0
187-2i	20.0			
187-23a	24.3			
187-31	28.5	1.29	2.56×10^{-2}	0
187-41	36.6			
187-41a	40.5	1.20	1.92×10^{-2}	0

III. RESULTS AND DISCUSSIONS

Fig. 4 shows the absorption coefficient α for various samples. The abscissa gives the excess donor concentration $N_D - N_A$ of the respective samples, temperature being the parameter. The absorption coefficient is obtained from the ratio of incident- and transmitted-radiation intensities measured, I/I_0 , and the relation $I/I_0 = (1 - R)^2 \exp(-\alpha d) / [1 - R^2 \exp(-2\alpha d)]$, where R is the reflectivity and d is the thickness of the sample. The denominator is replaced by 1 except for two samples with the lowest concentrations, because for other samples $ad > 2$ and the effect of multiple reflections and interference in the crystal is negligible. The value of reflectivity is determined by $R = (n - 1)^2 / (n + 1)^2$ setting $n = 4$ [15], where n is the refractive index of pure Ge. The value of R thus determined has been found adequate up to the concentration $N_D - N_A = 1 \times 10^{17} \text{ cm}^{-3}$ by means of I/I_0 measurements varying the thickness of the sample.

The absorption coefficient rapidly increases with the donor concentration showing a hump at around 3×10^{16}

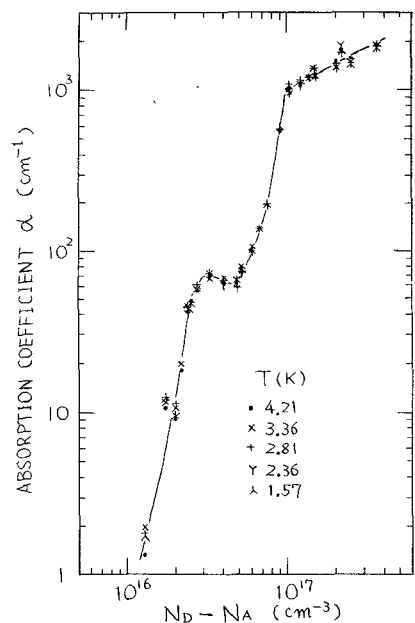


Fig. 4. Absorption coefficient of 337- μm radiation for various samples.

cm^{-3} , and is substantially independent of temperature below 4.2 K. The hump corresponds to the absorption associated with the activation energy ϵ_2 , as will be discussed later.

For the samples in the highest concentration region, the reflectivity increases from 0.36, the value determined previously, up to about 0.75 [16], indicating the effect of free carriers. The correction for the value of α is at most -10 percent if $R = 0.75$ is used to obtain α from measured I/I_0 . The values of α are close to the absorption coefficient derived from a free-carrier model.

The sharp increase of α in the region $7 \times 10^{16} \text{ cm}^{-3} < N_D - N_A < 1 \times 10^{17} \text{ cm}^{-3}$ is understood in terms of the transitions into the conduction band whose bottom is lowered [17] due to the interaction between donors.

In Fig. 5 the absorption cross section of 337- μm radiation is plotted against the activation energy ϵ_2 for the respective samples. The absorption cross section σ is obtained from the relation $\sigma = \alpha/N_D$, where the donor concentration N_D is replaced by $N_D - N_A$ in the present case because $N_A \ll N_D$.

For the samples with ϵ_2 larger than 3.7 meV, the photon energy $\hbar\omega$ of 337- μm radiation, σ falls rapidly with increasing ϵ_2 . For the samples with ϵ_2 smaller than $\hbar\omega$, σ passes through a maximum which corresponds to the hump in α in Fig. 4, and then decreases to about 60 percent of the maximum value showing a minimum as ϵ_2 is reduced, followed by a rapid increase accordingly as ϵ_2 approaches zero.

The measurement of the resistivity at temperatures below 4.2 K indicates that most of electrons associated with the donor impurities occupy the ground states. The photon energy is not enough for transitions from the ground state to excited states of the isolated donor, as has been seen in Fig. 2. The possibilities of phonon-assisted

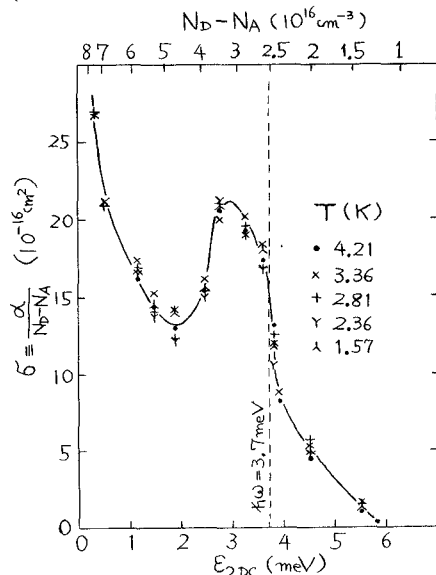


Fig. 5. Absorption cross section versus ϵ_2 for various samples. The upper scale gives the excess donor concentration.

transitions between these states [18], [19] and of the absorption associated with the free carriers thermally excited are ruled out because of the poor temperature dependence of σ . The fact that σ is not a monotonic increasing function of $N_D - N_A$ is difficult to be explained in terms of the transitions associated with tail states extended below the conduction band, since the absorption caused by the tail states shows an exponential dependence on the photon energy [20], [21]. The sharp increase in σ at $\epsilon_2 = \hbar\omega$ suggests that the absorption is due to the transition from the donor ground state to a delocalized conducting state which lies between the donor ground state and the conduction band, and that ϵ_2 is the energy needed for the transition.

The width of the peak of σ versus the ϵ_2 curve is about 1 meV. Provided that for the delocalized state a rigid-band model is valid in the narrow concentration range where the peak is observed, and that the coulomb interaction between an empty donor and a charge carrier in the delocalized state is neglected, the absorption cross section should reflect the density of states; the width should correspond to the bandwidth. On the other hand, when the coulomb potential is not negligible compared with the bandwidth, the absorption cross section does not reflect the state density but the absorption at the bottom of the band is enhanced [22]. The width of the peak shown in Fig. 5 seems too small to assure the one-electron interpretation for the present observation. The narrow width indicates an appreciable effect of coulomb interaction in the delocalized conducting state.

Fig. 6 shows the photoconductive response $-\Delta\rho/\rho$, a relative increase in the electrical conductivity on incidence of a unit photon flux, plotted against ϵ_2 for various samples. The samples are the same ones used for the measurement of absorption. The value of $-\Delta\rho/\rho$ is obtained from the relation $-\Delta\rho/\rho = -\Delta v/v \cdot \alpha d/[1 - \exp(-\alpha d)] \cdot \hbar\omega/I_i$ and observed v , Δv , and α , where v is the dc voltage

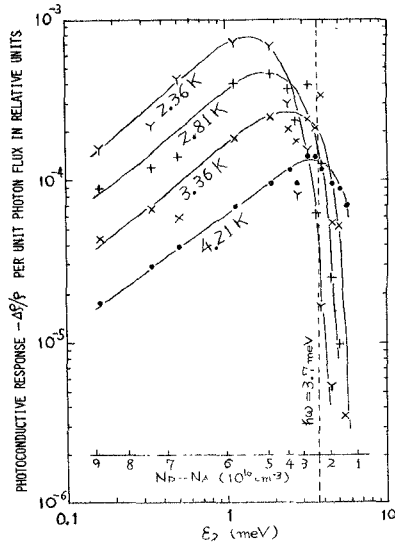


Fig. 6. Photoconductive response versus ϵ_2 .

across the sample, Δv is the ac (20-Hz) voltage produced on illumination, and $I_i/\hbar\omega$ is the photon-flux density just inside the illuminated surface. The factor $\alpha d/[1 - \exp(-\alpha d)]$ is introduced to take into account the damping of the incident power of radiation inside the sample. If $\alpha d \ll 1$, $-\Delta\rho/\rho$ tends to $-\Delta v/v \cdot \hbar\omega/I_i$. If $\alpha d \gg 1$, $-\Delta\rho/\rho$ tends to $-\Delta v/v \cdot \alpha d \cdot \hbar\omega/I_i$, then the conductivity changes only $1/\alpha$ in depth below the illuminated surface.

For $\epsilon_2 > 3.7 \text{ meV}$, $-\Delta\rho/\rho$ rapidly decreases with increasing ϵ_2 and also with falling temperature. The rapid decrease in $-\Delta\rho/\rho$ with ϵ_2 reflects decreases in α and the quantum yield, and indicates that the photon energy is not enough for the transition from the donor ground state to the delocalized state. This result confirms that the observed absorption is due to the transition into the delocalized state.

ACKNOWLEDGMENT

The authors wish to thank J. Kondo, K. Yamaji, H. Sumi, and S. Ogawa for helpful discussions. They also wish to thank Prof. W. Sasaki and Prof. T. Kurosawa for stimulating discussions.

REFERENCES

- [1] H. Fritzsche, "Resistivity and Hall coefficient of antimony doped germanium at low temperatures," *J. Phys. Chem. Solids*, vol. 6, pp. 69-80, July 1959.
- [2] C. Yamanouchi, "Effect of magnetic field on the intermediate impurity conduction in n-type germanium," *J. Phys. Soc. Jap.*, vol. 18, pp. 1775-1784, Dec. 1963.
- [3] —, "Hall coefficient and resistivity in the intermediate impurity conduction of n-type germanium," *J. Phys. Soc. Jap.*, vol. 20, pp. 1029-1034, June 1965.
- [4] O. N. Tufts and E. L. Stelzer, "Magnetoresistance in heavily doped n-type silicon," *Phys. Rev.*, vol. 139, pp. A265-A271, July 1965.
- [5] C. Yamanouchi, K. Mizuguchi, and W. Sasaki, "Electric conduction in phosphorus doped silicon at low temperatures," *J. Phys. Soc. Jap.*, vol. 22, pp. 859-864, Mar. 1967.
- [6] G. Sadasiv, "Magnetoresistance in germanium in the impurity conduction range," *Phys. Rev.*, vol. 128, pp. 1131-1135, Nov. 1962.
- [7] H. Fritzsche, "Effect of uniaxial compression on impurity conduction in n-type germanium," *Phys. Rev.*, vol. 125, pp. 1552-1567, Mar. 1962.
- [8] B. G. Zurkin, I. V. Kucherenko, and N. A. Penin, "Influence of uniaxial compression on hopping conduction in p-type Si,"

Sov. Phys.—Solid State, vol. 8, pp. 2767–2768, May 1967.

[9] T. Ishiguro and N. Mikoshiba, "Ultrasonic attenuation near the metal-nonmetal transition in n-Ge," in *Proc. 10th Int. Conf. Physics of Semiconductors* (Cambridge, Mass., 1970), pp. 569–574.

[10] J. Kinoshita, C. Yamanouchi, and K. Yoshihiro, "Far-infrared photoconductivity in phosphorus doped n-type silicon in the intermediate impurity concentration region under uniaxial compressional stress," *J. Phys. Soc. Jap.*, vol. 36, p. 1493, May 1974.

[11] W. Sasaki, "Low mobility states in highly compensated germanium," in *Proc. 10th Int. Conf. Physics of Semiconductors* (Cambridge, Mass., 1970), pp. 583–588.

[12] E. A. Davis and W. Dale Compton, "Compensation dependence of impurity conduction in antimony-doped germanium," *Phys. Rev.*, vol. 140, pp. A2183–A2194, Dec. 1965.

[13] K. Yoshihiro and C. Yamanouchi, "A stable cw HCN laser," *Rev. Sci. Instrum.*, pp. 767–768, June 1974.

[14] D. E. Williamson, "Cone channel condenser optics," *J. Opt. Soc. Amer.*, vol. 39, pp. 712–715, Oct. 1952.

[15] K. Lark-Horovitz and K. W. Meissner, "The optical properties of semiconductors. I. The reflectivity of germanium semiconductors," *Phys. Rev.*, vol. 76, p. 1530, Nov. 1949.

[16] K. Yoshihiro, M. Tokumoto, and C. Yamanouchi, "Far-infrared reflectivity of antimony doped germanium in the impurity concentration region," to be published.

[17] N. A. Penin, B. G. Zurkin, and B. A. Volkov, "Influence of the concentration of donors and acceptors on the electrical conductivity of heavily doped n-type silicon," *Sov. Phys.—Solid State*, vol. 7, pp. 2580–2584, May 1966.

[18] T. M. Lifshits and F. Ya. Nad', "Photoconductivity in germanium doped with group V impurities at photon energies below the impurity ionization energy," *Sov. Phys.—Dokl.*, vol. 10, pp. 532–533, Dec. 1965.

[19] Sh. M. Kogan and B. I. Sedunov, "Photothermal ionization of an impurity center in a crystal," *Sov. Phys.—Solid State*, vol. 8, pp. 1898–1903, Feb. 1967.

[20] D. L. Wood and J. Taue, "Weak absorption tails in amorphous semiconductors," *Phys. Rev.*, vol. 5, pp. 3144–3151, Apr. 1972.

[21] E. V. Burtsev, "On the theory of optical absorption spectra of disordered semiconductors," *Phys. Status Solidi B*, vol. 51, pp. 241–250, May 1972.

[22] M. Okazaki, M. Inoue, Y. Tovozawa, T. Inui, and E. Hanamura, "Coexistence of local and band characters in the absorption spectra of solids. II. Calculation for the simple cubic lattice," *J. Phys. Soc. Jap.*, vol. 22, pp. 1349–1361, June 1967.

High Pressure Far Infrared Spectroscopy of Ionic Solids

R. P. LOWNDES

Abstract—A high pressure far infrared cell operating to truly hydrostatic pressures of 8 kbar is described and used to determine the anharmonic self-energies associated with the $q \approx 0$ transverse optic modes of ionic solids.

I. INTRODUCTION

HIGH pressure far infrared studies can provide crucial information in many research areas including studies of anharmonicity in solids, studies of phase and ferroelectric transitions, and studies of defects in solids. If meaningful information is to be obtained from such researches, however, then it is clear that the high pressures must be applied hydrostatically. Unfortunately, far infrared studies under truly hydrostatic pressures are difficult primarily because of the lack of a readily available window material which satisfies the competing demands of strength and transmissivity in the far infrared. To date, much of the very limited far infrared high pressure research has been confined to work achieved with the opposed diamond anvil system [1]. However, reliable measurements are difficult to perform with this instrument due to the in-

herent difficulties of eliminating the pressure gradients generated across the opposed anvil faces and of accurately determining the system operating pressure. The consequences of these problems are that it is difficult to precisely determine the pressure dependence of mode eigenfrequencies and it is virtually impossible to reliably measure their spectral linewidths as a function of pressure using the diamond anvil system. In this paper we describe a high pressure far infrared cell which goes some way to solving these problems and which allows far infrared studies in the spectral range below 120 cm^{-1} for hydrostatic pressures up to 8 kbar. We describe investigations using this cell to determine the mode Gruneisen constants and the pressure dependence of the inverse lifetimes of the $q \approx 0$ transverse optic modes of RbI, CsI, and TiCl and use these measurements to investigate the complex anharmonic self-energy of these modes.

II. HIGH PRESSURE FAR INFRARED CELL

The high pressure far infrared cell used in these investigations is illustrated in Fig. 1. The cell body, window mounts, and retaining closures were machined from 4340 alloy steel and then heat treated to a hardness of RC 50 giving a yield strength of 14 kbar. The critical bores and surfaces of the cell and its components were ground and honed to size after the hardening process. Fully assembled, the cell had an effective speed of $f/2.4$.

Manuscript received May 6, 1974. This work was supported by a grant from the Army Research Office, Durham, N.C., and by grants from the National Science Foundation and the Research Corporation.

The author is with the Department of Physics, Northeastern University, Boston, Mass. 02115.